Advanced numerical modeling

New Horizons in Earth Reinforcement – Otani, Miyata & Mukunoki (eds)
© 2008 Taylor & Francis Group, London, ISBN 978-0-415-45775-0

Anisotropy of fiber-reinforced soil and numerical implementation

R.L. Michalowski
University of Michigan, Ann Arbor, U.S.A

ABSTRACT: While reinforcement in form of geosynthetic sheets or metal strips is used predominantly to improve structural integrity of the retaining walls, highway embankments, etc., short fiber reinforcement can be used to improve properties of the soil used as fill in geotechnical structures. A development of an anisotropic yield condition for fiber-reinforced sand is presented. As the composite's properties are anisotropic, the traditional kinematic approach of limit analysis needs to be modified to account for anisotropy. An example is shown where fiber-reinforced sand is used as backfill behind a retaining wall.

1 INTRODUCTION

Estimates of contribution of short fibers to the soil strength were made earlier for isotropic reinforced soils where the orientation of fibers was distributed evenly in all directions (Michalowski & Zhao 1996, Michalowski & Čermák 2003). Because of the technology of deposition of fiber-reinforced soils (mixing and compacting), the orientation of fibers has clearly a preferred bedding plane, giving rise to anisotropy of mechanical properties of the mixture. The research presented in this paper is concentrated on anisotropy of the strength properties, and on application of limit analysis to anisotropic fiber-reinforced sand.

The interest in fiber reinforcement of soils began in the 1970's with an attempt to estimate the influence of the plant/tree roots on stability of earth slopes (Walderon 1977). Subsequent models were based on analysis of a single fiber intersecting a band of soil with localized shear strain (Gray & Ohashi 1983, Maher & Gray 1990. While these efforts revealed the complexity of the soil-fiber interaction, they did not produce a yield condition in terms of the components of the stress tensor. Consequently, the early models were not implemented in the numerical tools, such as the finite element method, or in the numerical optimization schemes used in kinematic approach of limit analysis.

A yield condition for fiber-reinforced soil with ellipsoidal distribution of the fiber orientation is presented here. The plastic state and the kinematic discontinuities in the deformation fields will be discussed. The internal friction angle of an anisotropic composite is dependent on the orientation (direction), and a method to extract this angle from the anisotropic yield condition will be presented. Finally, an application example will be shown.

2 DEVELOPMENT OF THE YIELD CONDITION

The distribution of fiber orientation is considered in a form of an ellipsoid (Fig. 1), with a preferred bedding plane xOz.

This distribution is axi-symmetric and is a function of angle θ

$$\rho(\theta) = \frac{ab}{\sqrt{a^2 \sin^2\theta + b^2 \cos^2\theta}} \tag{1}$$

where a and b are the half-axes of the distribution. For convenience, the distribution aspect ratio is introduced, defined as

$$\xi = \frac{b}{a} \tag{2}$$

The total content of fibers is defined by their average concentration $\bar{\rho}$

$$\overline{\rho} = \frac{V_r}{V} \tag{3}$$

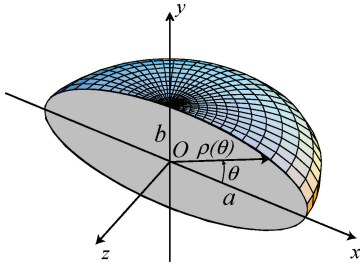

Figure 1. Ellipsoidal distribution of fiber orientation.

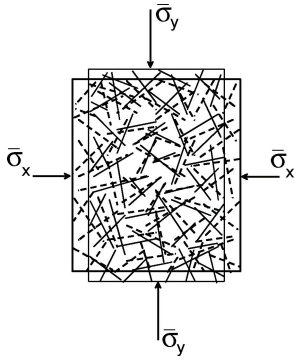

Figure 2. Deformation of a representative element.

where V_r and V are the volume of fibers and the volume of the representative element, respectively. The aspect ratio η of the cylindrical fibers of length l and radius r is defined as

$$\eta = \frac{l}{2r} \tag{4}$$

The yield condition is developed using a homogenization method where an incipient plastic deformation process is considered, as in Figure 2.

It is required that the internal work $D(\dot{\varepsilon}_{ij})$ in the representative element be balanced by the work of the average (macroscopic) stress $\bar{\sigma}_{ij}$ on the boundaries of the element

$$\bar{\sigma}_{ij}\dot{\bar{\varepsilon}}_{ij} = \frac{1}{V}\int_V D(\dot{\varepsilon}_{ij})\,dV \tag{5}$$

The internal work is dissipated in the irreversible process, and it is due to the frictional slip of the fibers in the matrix material (sand). Because the composite is anisotropic, the principal directions of the stress and strain rates, in general, do not coincide.

Calculations of the internal work rate in eq. (5) are tedious, and the details are omitted here (relevant earlier research can be found in di Prisco & Nova 1993, Michalowski 1997, Michalowski and Čermák 2002). The yield condition is sought in the following form

$$f = R - F(p,\psi) = 0 \tag{6}$$

where R is the maximum shear stress

$$R = \frac{1}{2}\left[(\bar{\sigma}_x - \bar{\sigma}_y)^2 + 4\bar{\tau}_{xy}^2\right]^{\frac{1}{2}} = \left(q^2 + \bar{\tau}_{xy}^2\right)^{\frac{1}{2}} \tag{7}$$

and p and ψ are the in-plane mean stress p ($p = (\bar{\sigma}_1 + \bar{\sigma}_3)/2$) and the angle that the major principal stress makes with axis x, respectively. Some numerical results are shown in Figure 3.

The contribution of fibers to the strength can be characterized as a function of total fiber content $\bar{\rho}$

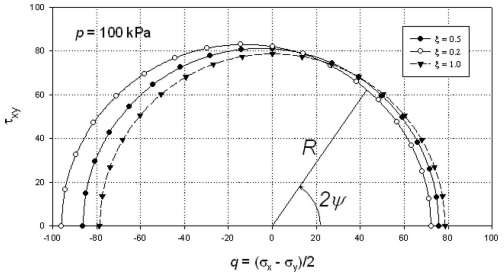

Figure 3. Calculated yield condition for fiber-reinforced sand.

(eq. (3)), distribution aspect ratio ξ (eq. (2)), fiber aspect ratio η (eq. (4)), angle of the sand-fiber interface friction ϕ_w, and also the internal friction angle of the sand (matrix material), ϕ. The analysis revealed that the number of independent parameters can be reduced to three: ϕ, product $\bar{\rho}\eta \tan\phi_w$, and ξ. The calculated yield surfaces in Figure 3 are for $p = 100$ kPa, $\phi = 36°$, $\bar{\rho}\eta \tan\phi_w = 0.89$, and 3 distribution ratios ξ: 0.2, 0.5, and 1.0 (isotropy).

It is interesting to notice that the trace of the yield surface at $p = \text{const}$ is approximately circular, independent of the distribution aspect ratio ξ. It is convenient then to approximate the yield function with a circle whose radius and the shift of the center along q-axis (Fig. 3) depend on internal friction angle of the sand ϕ, product $\bar{\rho}\eta \tan\phi_w$ characterizing the fibers, and ratio ξ that carries information about the anisotropic fiber orientation distribution.

3 LIMIT ANALYSIS WITH ANISOTROPIC SOIL

3.1 *Anisotropic yield condition*

Kinematic approach of limit analysis has been used often in geotechnical engineering, but the applications have been limited predominantly to isotropic soils. However, the distribution of the fibers in Figure 1 leads clearly to an anisotropic composite. For constant mean stress p, the trace of the yield condition for the fiber-reinforced soil can be conveniently represented as a circle; this is confirmed by the numerical homogenization calculations that led to the yield contours in Figure 3. For an isotropic distribution of fibers, $\xi = 1.0$, the yield condition can be graphically represented as a circle with its center at the origin of coordinate system q, τ_{xy} (Fig. 3).

The calculations indicated that for anisotropic distribution of the fibers the yield condition can still be represented by a circle, but this circle is now shifted along axis q by distance Q, as indicated in Figure 4.

The maximum shear stress R is now different from the radius of the circle R_0, and it is dependent on inclination angle ψ of the major principal stress, which

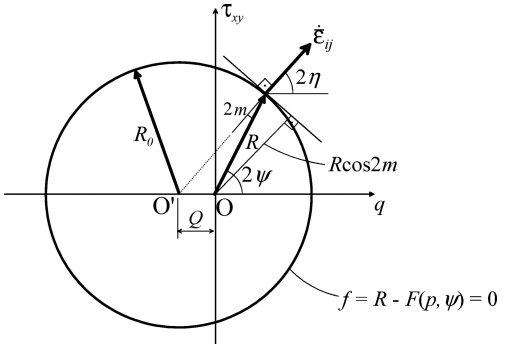

Figure 4. Anisotropic yield condition for fiber-reinforced sand.

Table 1. R_0/p and Q/p for anisotropic fiber-reinforced sand.

ϕ	$\bar{\rho}\eta \tan \phi_w$	ξ	R_0/p	Q/p
30°	0.20	1.0	0.5406	0
		0.5	0.5456	0.0110
		0.2	0.5524	0.0251
	0.40	1.0	0.5812	0
		0.5	0.5912	0.0220
		0.2	0.6048	0.0502
35°	0.20	1.0	0.6175	0
		0.5	0.6228	0.0116
		0.2	0.6298	0.0265
	0.40	1.0	0.6614	0
		0.5	0.6721	0.0233
		0.2	0.6861	0.0530

is characteristic of anisotropy. It is also clear from Figure 4 that the principal directions of the macroscopic stress and strain rate tensors do not coincide: $2\eta \neq 2\psi$ (normality rule is used to describe the deformation rate).

For practical purposes it is convenient to represent the radius R_0 and the shift Q as functions of angle ϕ, coefficient $\bar{\rho}\eta \tan \phi_w$, and distribution ratio ξ. A sample of the calculation results is given in Table 1. The results for $\xi = 1.0$ represent the yield condition of isotropic fiber-reinforced soil, with shift $Q = 0$. Since function $F(p, \psi)$ in eq. (6) is a linear and homogeneous function of p, the results in Table 1 are given as ratio R_0/p and Q/p.

3.2 *Evaluation of yield surface parameters*

This paper relates only to the theoretical aspects of the model and analysis. However, the parameters of the yield condition can be validated experimentally. Two plane-strain compression tests are needed to estimate R_0 and Q, one with the major principal stress perpendicular to the plane of fiber preferred orientation, and the second one with the major principal stress coinciding with the trace of the preferred bedding plane. Consequently, maximum and minimum of q on the yield surface in Fig. 4 can be determined, and R_0 and Q (or R_0/p, Q/p) evaluated, since the trace of the yield condition was approximated as a circle. In practice, more than two tests are needed, to assure repeatability of the results.

3.3 *Mechanisms with velocity discontinuities*

Kinematic approach of limit analysis requires consideration of velocity discontinuities, since they are part of admissible failure mechanisms. It can be demonstrated that the differential equations describing the plastic stress field and the plastic deformation are of hyperbolic type (Booker & Davis 1972). Similar to the isotropic case, the characteristics of the two sets of equations coincide (normality flow rule is used), but their analytical representation differs slightly for anisotropy

$$\frac{dy}{dx} = \tan(\psi - m \pm \nu) = \tan(\eta \pm \nu), \qquad \alpha, \beta \tag{8}$$

where angles m, η and ψ are illustrated in Figure 4, angle ν for the soil with linear dependence on p becomes

$$\nu = \frac{\pi}{4} - \frac{\phi_a}{2} \tag{9}$$

It follows from kinematics considerations that velocity discontinuities must coincide with velocity characteristics, and the dilatancy along these discontinuities is governed by internal friction angle ϕ_a. However, angle ϕ_a is dependent on orientation of the characteristic line. In kinematic approach of limit analysis the geometry of velocity discontinuities is not given *a priori*, but their inclination is subject to variation in search for the best bound to the limit load. Therefore, angle ϕ_a also will vary in the numerical procedure. Calculations of angle ϕ_a as function of orientation (direction) are illustrated in the next subsection.

3.4 *Internal friction angle in anisotropic soil*

For isotropic material the internal friction angle ϕ is independent of ψ

$$\sin \phi = \frac{R_0}{p} \tag{10}$$

Internal friction angle ϕ_a for anisotropic composite is not a constant, and it varies with the change in the physical orientation (direction). The relation among ϕ_a, R and p now becomes

$$\sin \phi_a = \frac{R \cos(2\psi - 2\eta)}{p} = \frac{R \cos 2m}{p} \tag{11}$$

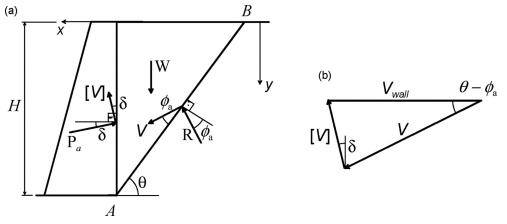

Figure 5. (a) Schematic of a retaining wall, (b) hodograph.

Table 2. Wall load coefficient K_a.

ϕ	δ	$\bar{\rho}\eta \tan \phi_w$	ξ	K_a
30°	15°	0	–	0.301
		0.20	1.0	0.271
			0.5	0.260
			0.2	0.245
		0.40	1.0	0.242
			0.5	0.221
			0.2	0.193

where angle $2m$ and the graphical interpretation of $R \cos 2m$ are shown in Fig. 4. Based on eq. (8), the characteristics (and therefore the velocity discontinuities) are inclined to axis x at angles $\eta \pm (\pi/4 - \phi_a/2)$, but angles η and ϕ_a are related through eq. (11). Hence the calculations of angle ϕ_a need to be iterative. A simple "classroom" example is presented in the next section.

4 EXAMPLE

This example relates to the problem of active backfill load on a retaining wall. It is expected that fiber reinforcement in a backfill will lead to reduction of the load. Of particular interest is how the anisotropy of fiber distribution affects the loads.

We consider a vertical but rough wall, Figure 5(a). The kinematic approach of limit analysis is used, and the hodograph for one-block (Coulomb-type) mechanism is shown in Figure 5(b). The roughness of the wall is included in calculations by assuming relative wall/soil motion vector [v] being inclined at interface friction angle δ to the wall.

The velocity discontinuity (or failure surface) AB is a characteristic of β-family, therefore its inclination angle θ can be related to the direction of the major principal strain rate η through eq. (8) as

$$\theta = \eta - \frac{\pi}{4} + \frac{\phi_a}{2} \tag{12}$$

In the process of finding the best solution to the wall loading, angle θ is varied until the maximum of pressure coefficient K_a is found (the kinematic approach yields the lower bound here, because force P_a is a reaction rather than an active force). The numerical results are presented in Table 2.

As the fibers reinforce the backfill, the load from the backfill on the wall is reduced, and this reduction increases with an increase in $\bar{\rho}\eta \tan \phi_w$. Significant reduction in the load on the wall for given amount of fibers is achieved by making the fiber distribution "more anisotropic" (reduction in the fiber distribution ratio ξ).

5 FINAL REMARKS

A model for fiber-reinforced soil with anisotropic distribution of orientation of fibers was developed, and application of the kinematic approach of limit analysis to anisotropic soils was presented. The method becomes more elaborate, compared to its application to isotropic soils, because the internal friction angle depends now on orientation. The method is effective in solving problems with anisotropic materials. A simple example of retaining wall with fiber-reinforced backfill was presented.

ACKNOWLEDGEMENT

The work presented in this paper was carried out while the author was supported by the Army Research Office, grant No. DAAD19-03-1-0063. This support is greatly appreciated.

REFERENCES

Booker, J.R. & Davis, E.H. 1972. A general treatment of plastic anisotropy under conditions of plane strain. *J. Mech. Phys. Solids* 20: 239–250.

Gray, D.H. & Ohashi, H. 1983. Mechanics of fiber reinforcement in sand. *J. Geot. Eng.*, 109: 335–353.

Maher, M.H. & Gray, D.H. 1990. Static response of sands reinforced with randomly distributed fibers. *J. Geot. Eng.*, Vol. 116(11): 1661–1677.

Michalowski, R.L. 1997. Limit stress for granular composites reinforced with continuous filaments. ASCE *Journal of Engrg. Mechanics*, 123(8): 852–859.

Michalowski, R.L. & Čermák, J. 2003. Triaxial compression of sand reinforced with fibers. *Journal of Geotechnical and Geoenvironmental Engineering*, 129(2): 125–136.

Michalowski, R.L. & Čermák, J. 2002. Strength anisotropy of fiber-reinforced sand. *Computers and Geotechnics*, 29(4): 279–299.

Michalowski, R.L. & Zhao, A. 1996. Failure of fiber-reinforced granular soils. *J. Geot. Geoenv. Engrg.*, ASCE, 122(3): 226–234.

di Prisco, C. & Nova, R. 1993. A constitutive model for soil reinforced by continuous threads. *Geotextiles and Geomembranes*, 12: 161–178.

Waldron, L.J. 1977. The shear resistance of root-permeated homogeneous and stratified soil. *Soil Sci. Soc. Am.*, 41: 843–849.